SpringerPlus
a SpringerOpen Journal

CASE STUDY Open Access

A case of post-transplant adult T-cell leukemia/lymphoma presenting myelopathy similar to but distinct from human T-cell leukemia virus type I (HTLV- I)-associated myelopathy

Toyotaka Kawamata[1*], Nobuhiro Ohno[1], Kota Sato[1,2], Masayuki Kobayashi[1,2], Norihide Jo[1], Koichiro Yuji[1], Ryuji Tanosaki[3], Yoshihisa Yamano[4], Arinobu Tojo[1,2] and Kaoru Uchimaru[1]

Abstract

Introduction: Adult T-cell leukemia/lymphoma (ATL) responds poorly to conventional chemotherapy, but allogeneic stem cell transplantation (allo-SCT) may improve disease prognosis. Herein, we report a female patient with human T-cell leukemia virus type I (HTLV-I)-associated myelopathy (HAM)-like myelopathy following allo-SCT for ATL.

Case report: She developed crural paresis 14 months after allo-SCT. Initially, she was diagnosed with central nervous system (CNS) relapse of ATL and treated with intrathecal injection and whole brain and spine irradiation. Her symptoms recurred 5 months later, when a cerebrospinal fluid (CSF) specimen showed increased CD4 + CXCR3 + CCR4+ cell numbers and levels of neopterin and CXCL10 (IP-10).

Discussion: These results suggest the possible involvement of a certain immunological mechanism such as HAM in her symptoms, irrespective of the lack of anti-HTLV-I antibody in her CSF. Because a definitive diagnosis of CNS manifestation of ATL is sometimes difficult, multi-modal laboratory data are required for differential diagnosis.

Keywords: Adult T-cell leukemia/lymphoma; Post-transplant myelopathy; HTLV-I-associated myelopathy (HAM); Neopterin; CXCL10 (IP-10)

Introduction

Human T-cell leukemia virus type I (HTLV-I) was the first retrovirus identified in humans, isolated from a patient with cutaneous lymphoma (Poiesz et al. 1980). HTLV-I is the cause of not only adult T-cell leukemia/lymphoma (ATL) (Uchiyama et al. 1977; Hinuma et al. 1981) but also HTLV-I-associated myelopathy (HAM)/tropical spastic paraparesis (TSP) (Osame et al. 1986), HTLV-I-associated uveitis (HU) (Ohba et al. 1989; Mochizuki et al. 1992) and infective dermatitis (McGill et al. 2012; de Oliveira et al. 2010).

ATL is one of the most intractable T-cell malignancies, and it responds poorly to conventional chemotherapy, with a median survival time (MST) of approximately 8 months (Shimoyama et al. 1988). Among such treatments, modified LSG-15 (mLSG-15) has shown the best results; in a previous study, the progression free survival (PFS) at 1 year among patients treated with mLSG-15 was 28% and the overall survival (OS) at 3 years was 24% (Tsukasaki et al. 2007). However, the improvement in survival time by mLSG-15 treatment is not satisfactory. Allo-HSCT is a promising treatment option to cure ATL because it may improve disease prognosis (Utsunomiya et al. 2001; Kami et al. 2003).

Herein, we describe a case of HAM-like myelopathy that was difficult to distinguish from central nervous system (CNS) relapse of ATL following allogeneic peripheral blood stem cell transplantation. This case report suggests that there might be immunological myelopathy after HSCT. In the present case, flow cytometric analysis of the cells in cerebrospinal fluid (CSF) was helpful to differentiate it from CNS relapse of ATL.

* Correspondence: toyotaka@ims.u-tokyo.ac.jp
[1]Department of Hematology/Oncology, Research Hospital, The Institute of Medical Science, the University of Tokyo, 4-6-1 Shirokanedai, Minato-ku, Tokyo 108-8639, Japan
Full list of author information is available at the end of the article

Case report

A 63-year-old female patient recognized cervical lymph nodes swelling in October 2010. Lactate dehydrogenase (LDH) and serum corrected calcium levels kept within normal limit, but soluble interleukin-2 receptor (sIL-2R) elevated significantly at the initial visit (Table 1). Diagnostic imaging by computed tomography (CT) revealed systemic lymphadenopathies (cervical, axial, mediastinal, abdominal and mesenteric lymphadenopathy) before the following chemotherapy. Although appetite loss and abdominal distention were added with lymphadenopathy, any other abnormal finding of physical examination could not be detected. Her ECOG performance status was grade 1 before chemotherapy. She received cervical lymph node biopsy and pathological findings of cervical lymph node revealed T cell lymphoma compatible, and HTLV-I provirus DNA analysis (Southern blot) revealed monoclonal integration. Abnormal lymphocytes were not detected in peripheral blood (PB) and HTLV-I provirus DNA analysis of PB did not show monoclonal integration. She was diagnosed as ATL (lymphoma type). She has past histories of glaucoma and pulmonary cryptococcosis. None of ATL patient was in her family.

She was referred to our hospital and received four sessions of mLSG-15 therapy in our hospital. Prophylactic intrathecal injection was performed twice, during chemotherapy and before allogeneic stem cell transplantation. No meningeal involvement of ATL cells was detected at that time. She went into complete remission (Response criteria for adult T cell leukemia-lymphoma from an international consensus meeting (Tsukasaki et al. 2009)) in April 2011. She received following allogeneic peripheral blood stem cell transplantation (allo-PBSCT) in the National Cancer Center Hospital (Tokyo, Japan) (Figure 1). The transplantation conditioning regimen consisted of fludarabine (30 mg/m^2 per day for 5 days) plus busulfan (3.2 mg/kg per day for 2 days) and only cyclosporine A (CyA) was used for GVHD prophylaxis. Transplanted CD34-positive cells were 2.67×10^6/kg and rapid engraftment was achieved. Grade III (gastrointestinal tract and skin) acute graft-versus-host disease (GVHD) was observed 1 month after transplantation, but it improved after treatment with methylpredonisolone (mPSL) (1 mg/kg). No chronic GVHD was observed. CyA was tapered gradually and discontinued 9 months after transplantation, in February 2012. After that point, only 5 mg/day predonisolone (PSL) was continued.

In July 2012 (14 months after allo-PBSCT), the patient developed hemiparesis of the left side. Although left upper-limb paresis improved, lower-extremity paresis progressed to paraplegia. Magnetic resonance imaging (MRI) revealed multiple high-intensity lesions in T2-weighted images of the medulla oblongata, cervical spinal cord, and thoracic spinal cord (Figure 2A), and a CSF specimen showed increased cell counts (Figure 3). Morphologically, typical ATL cells such as flower cells were not detected in CSF, but abnormal small to middle size lymphocytes indistinguishable from ATL cells increased. She was diagnosed as CNS relapse of ATL, and received mPSL pulse, intrathecal injection of MTX 15 mg + Ara-C 40 mg + PSL 20 mg, and irradiation of the whole brain and spine. Following these treatments, the paraplegia improved gradually to such a degree that she could walk with a walker. During the course of these treatments, she was complicated by neurogenic bladder dysfunction, and diabetes insipidus.

In January 2013 (20 months after allo-PBSCT), she again developed left lower-limb weakness, which gradually progressed. She was admitted to our hospital in February 2013. On admission, neurological examination revealed

Table 1 Laboratory data of onset of ATL (lymphoma type) in October 2010

WBC	4100/μl	GOT	67 IU/L	CRP	0.06 mg/dl
Myelo	1.0%	GPT	72 IU/L	sIL-2R	5802 U/ml
St	8.0%	LDH	215 IU/L		
Seg	71.0%	ALP	277 IU/L	HTVL-I Ab	(+)
Ly	11.0%	γ-GTP	46 IU/L	HBs-Ag	(−)
Mo	8.0%	Alb	3.5 mg/dl	HBs-Ab	(−)
Baso	1.0%	BUN	15.6 mg/dl	HBc-Ab	(−)
RBC	423×10^4/μl	Cre	0.58 mg/dl	HCV-Ab	(−)
Hb	13.2 g/dl	Na	142.4 mEq/L	HIV-Ab	(−)
Hct	39.0%	K	4.2 mEq/L	TPHA	(−)
MCV	92.2 fl	Cl	103.8 mEq/L		
MCH	31.2 pg	Corrected Ca	9.9 mg/dl		
MCHC	33.8%				
Plt	21.9×10^4/μl				

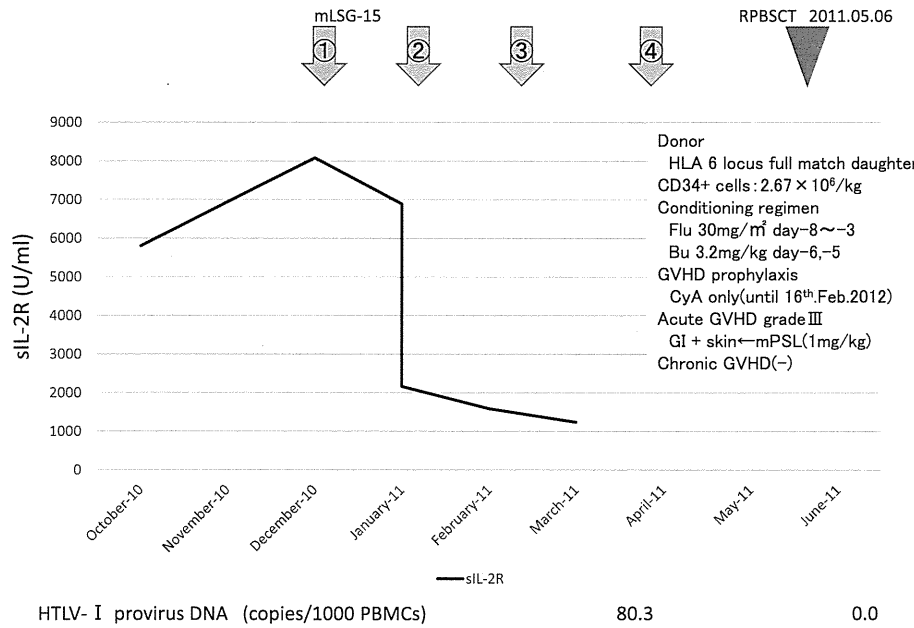

Figure 1 Clinical course from conventional chemotherapy (mLSG-15) to allogeneic peripheral blood stem cell transplantation. The patient received four sessions of mLSG-15 therapy and achieved complete remission (CR) before receiving allo-PBSCT.

no abnormality of cranial nervous system, but abnormal reflex such as Babinski and Chaddock reflex in bilateral lower-limb. Thermal hypoalgesia under right Th4 and left Th6 dermatome was detected, but tactile sense was intact. She was accompanied with bladder dysfunction and severe constipation. Brain and spinal MRI revealed a residual spinal lesion at Th3-7 (Figure 2B). The cell numbers in CSF did not increase, but myelin basic protein (MBP) level was elevated (Figure 4B). Morphologically, ATL cells could not be detected in CSF. Flow cytometric analysis to determine the specific immunophenotype of CD4+ lymphocytes in CSF revealed an expansion of the $CD4^+CXCR3^+CCR4^+$

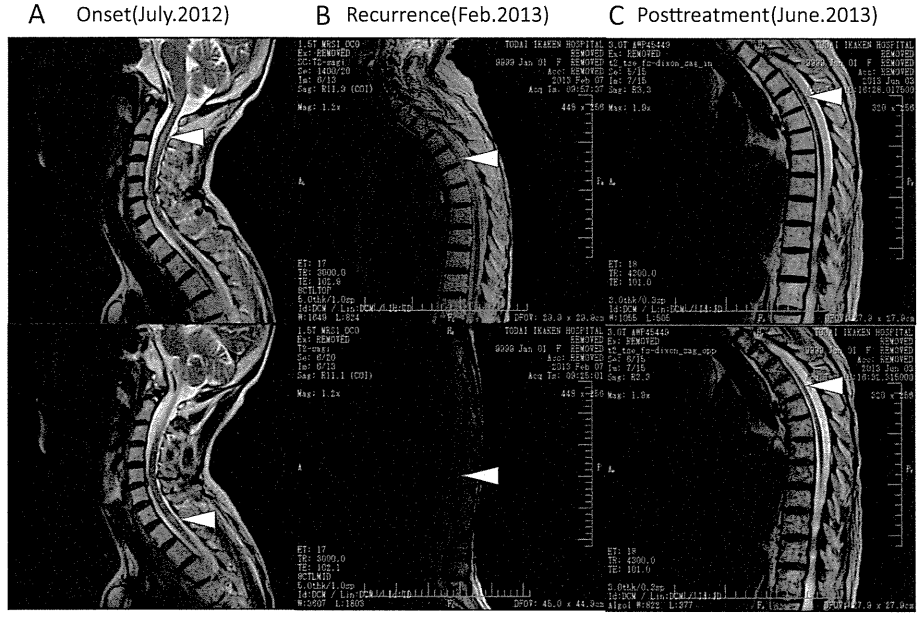

Figure 2 MRI findings. A) At the onset of neurogenic disorder in July 2012. Multiple high-intensity lesions in T2-weighted images (T2WI) of the medulla oblongata, cervical spinal cord, and thoracic spinal cord were revealed. **B)** Residual high-intensity lesion in Th3-7. **C)** Following treatment, the residual lesion in the thoracic spinal cord improved.

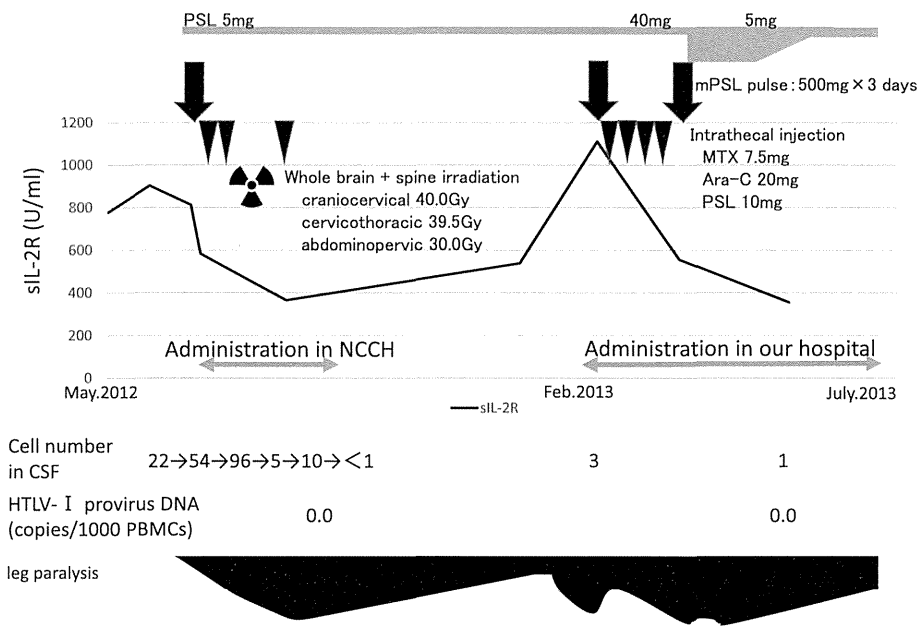

Figure 3 Clinical course after onset of the neurogenic disorder. The patient developed paraplegia 14 months after allo-PBSCT. Neurological findings were partially relieved following treatment with a high dose of mPSL accompanied by intrathecal injection of MTX + Ara-C + PSL and irradiation of the whole brain and spine. Three months later, her neurological deficit worsened again. Ultimately, her neurological disorder improved after treatment with a high dose of steroid.

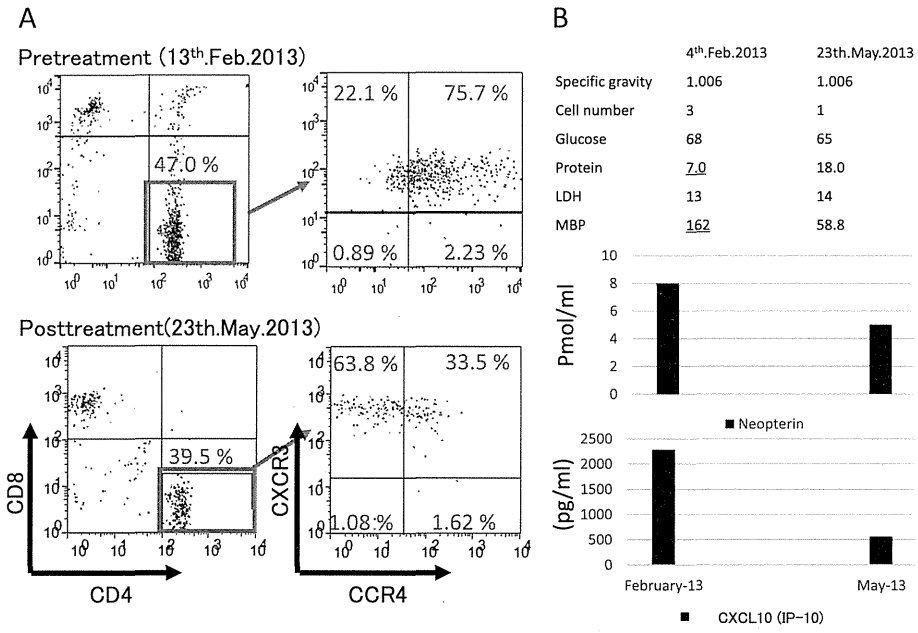

Figure 4 CSF findings. A) Flow cytometric analysis of CSF. Before treatment, the CD4 + CXCR3 + CCR4+ cell population was predominantly elevated. Following treatment, it decreased and the CD4 + CXCR3 + CCR4- cell population increased. **B)** Neopterin and CXCL10 (IP-10) concentrations in CSF. Before treatment, both neopterin and CXCL10 (IP-10) concentrations were significantly elevated. Following treatment, both biomarkers decreased to within the range of the therapeutic goal for HAM patients.

cell population (Figure 4A), which conflicted with CNS relapse of ATL but was consistent with HAM (Natsumi et al. 2014). Furthermore, both the neopterin and CXCL10 (IP-10) concentrations in the CSF were significantly elevated (Figure 4B), although lower than those associated with aggressive HAM (14). Notably, the case was insufficient to fulfill the diagnostic criteria for HAM (Mitsuhiro 1990) because HTLV-I antibody (PA method) was negative in CSF.

Bacterial, fungal, and tuberculous encephalomyelopathies were excluded because no increase in cell numbers and no decline in glucose concentration in CSF were observed. Real-time polymerase chain reaction (PCR) testing for CMV, EBV, HSV, VZV, HHV-6, and JC virus in CSF showed negative results.

Serum soluble interleukin-2 receptor (sIL-2R) level was slightly elevated (Table 2), but significantly lower compared with that at the onset of ATL.

Not all of the results necessarily corresponded to CNS relapse of ATL, although we could not exclude it. We treated her with mPSL pulse and intrathecal injection of MTX + Ara-C + PSL. After one course of mPSL pulse, her crural paresis improved dramatically to such a degree that she could pull up to standing after a few days. Although she was given intrathecal injections four times weekly, her crural paresis was gradually exacerbated and progressed to paralysis. mPSL pulse was performed again, but the effect was limited.

We examined her CSF again but there was no increase in cells, and ATL cells could not be detected by microscopic examination. Furthermore, the MRI findings improved over time (Figure 2C), although her neurological findings worsened and HTLV-I proviral DNA could not be detected repeatedly in peripheral mononuclear cells (PBMCs) after allo-PBSCT. No evidence of relapsed ATL could be found and we continued 5 mg/day PSL thereafter while she continued rehabilitation.

The results of CSF analysis in May 2013 showed the following improvements. In flow cytometric analysis, the CD4 + CXCR3 + CCR4+ cell population had decreased and the normal CD4 + CXCR3 + CCR4- cell population had increased. Both neopterin and CXCL10 (IP-10) had decreased to within the range of the therapeutic goal for HAM patients (Figure 4A,B). Her paralysis improved gradually and steadily only by rehabilitation, to such a degree that she could walk when holding onto parallel bars.

Discussion

ATL with CNS involvement may occur during systemic progression of the disease and its frequency is estimated to be 10–25% (Kitajima et al. 2002). However, cases of CNS relapse without peripheral blood and lymph nodes of ATL have been reported (Marshall et al. 1998; Dungerwalla et al. 2005). In flow cytometric analysis of CSF of ATL patients, the CD4 + CXCR3-CCR4+ cell population is elevated. However, in the current case, the CSF fluid analysis revealed expansion of the CD4 + CXCR3 + CCR4+ cell population, which is consistent with HAM (Natsumi et al. 2014). Sato T et al. (Sato et al. 2013) reported increased neopterin and CXCL10 (IP-10) in HAM patients, and they were valuable biomarkers for disease progression of HAM. The neopterin and CXCL10 (IP-10) concentration in CSF paralleled the disease activity of HAM. The cut-off concentrations of neopterin and CXCL10 in HAM/TSP patients compared to HTLV-I infected non-HAM subjects are less than 5 pmol/mL and 200 pg/ml, respectively, and the CXCL10 (IP-10) concentration in the CSF of HAM patients with rapid progression is usually more than 5,000 pg/mL (Yamono, Y., personal communication). In the current case, we could not make a diagnosis of HAM because the CSF was negative for HTLV-I antibody in repeated examinations. Although the immunosuppressive status after allo-PBSCT might contribute, serum immunoglobulin levels

Table 2 Laboratory data on admission to our hospital in January 2013

WBC	4470/μl	GOT	15 IU/L	CRP	0.24 mg/dl
St	1.5%	GPT	33 IU/L	IgG	1390 mg/dl
Seg	64.0%	LDH	199 IU/L	IgA	51 mg/dl
Ly	14.0%	ALP	453 IU/L	IgM	352 mg/dl
Mo	19.5%	γ-GTP	87 IU/L		
Abnormal Ly	1.0%	TP	6.7 mg/dl	HTVL-I Ab	(+)
RBC	302×10^4/μl	Alb	3.5 mg/dl	HBs-Ag	(–)
Hb	9.5 g/dl	BUN	9.8 mg/dl	HBs-Ab	(–)
Hct	29.4%	Cre	0.56 mg/dl	HBc-Ab	(–)
MCV	97.4 fl	Na	133 mEq/L	HCV-Ab	(–)
MCH	31.5 pg	K	4.0 mEq/L	HIV-Ab	(–)
MCHC	32.3%	Cl	96 mEq/L		
Plt	12.0×10^4/μl	Corrected Ca	10.5 mg/dl		

were almost within normal limit at the same time period (Table 2) and there is not enough evidence to indicate false negative. In any inflammatory diseases of CNS, CXCR3+ cells but not CCR4+ cells were generally found in CSF (Misu et al. 2001). However, CXCR3 + CCR4+ double positive cells existed in her CSF. It was unlikely that CXCR3 + CCR4+ double positive cells emerged into CSF in nonspecific inflammatory condition. Given her background, we supposed these CCR4+ cells were HTLV-I infected cells, but the number of these cells was insufficient to measure HTLV-I viral load.

In the current case, neither CSF data nor clinical course consisted with CNS relapse of ATL. In case of ATL patients, CXCR3-CCR4+ T cell lymphocytes population expanded. Therapeutic effect was obtained from mPSL pulse rather than intrathecal injection. Furthermore, disease progression in the typical case of CNS relapse of ATL was more aggressive. We concluded some inflammatory condition caused by these HTLV-I infected cells may have developed HAM-like myelopathy.

CNS GVHD remains a controversial entity and it is difficult to establish an unequivocal diagnosis. Yet a few cases have been reported, who were suspected of CNS GVHD from brain biopsy or autopsy, their CSF showed predominant T-lymphocyte infiltration of donor origin (Kamble et al. 2007). In the current case, brain or spinal cord biopsy was not performed, and chimerism analysis of T cells in CSF was difficult because of the full-match HLA and sex-matched PBSCT. The number of T cells in CSF was insufficient to analyze chimerism using the short tandem repeat (STR) method. Neopterin (Niederwieser et al. 1984; Hempel et al. 1997) and CXCL10 (IP-10) (Mapara et al. 2006) levels in serum increase significantly in patients with active GHVD, but the levels in CSF are unknown. The possibility of active CNS GVHD could not be completely excluded. Both CXCR3 and CCR4 expression of T cells infiltrated in the CNS in patients with active CNS GVHD is unknown. It was no wander that CXCR3+ cells in CSF were found in nonspecific inflammatory condition such as CNS GVHD, but unlikely that CCR4+ cells were.

The patient's neurological dysfunction seemed to fluctuate in parallel with the serum concentration of soluble interleukin-2 (sIL-2R) receptor (Figure 3). However, increased sIL-2R occurs not only with ATL relapse but also with HAM (Matsumoto et al. 1990), GVHD (Kami et al. 2000), and inflammatory neurogenic disorders caused by immunologic T-cell responses (Maier et al. 2009). Thus, it is difficult to make a definite diagnosis based on elevated sIL-2R alone.

In conclusion, we report a case with myelopathy without ATL relapse in the CNS. Flow cytometric analysis is helpful to differentiate immune-mediated encephalopathy or myelopathy from CNS relapse of ATL. If we encountered the patients suspected of CNS relapse of ATL, we should consider the possibility of inflammatory condition caused by HTLV-I infected cells. Further analysis of pathology are warranted.

Competing interests
The authors declare that they have no competing interests.

Authors' contribution
TK participated in treatment for the patient and drafting the manuscript. NO, KS, MK, NJ and KY participated in treatment for the patient. YY carried out flow cytometric analysis and measurement of neopterin and CXCL10 (IP-10) concentration in CSF, and helped to draft the manuscript. RT participated in acquiring the data and helping to draft the manuscript. AT and KU supervised and helped to draft the manuscript. All authors read and approved the final manuscript.

Author details
[1]Department of Hematology/Oncology, Research Hospital, The Institute of Medical Science, the University of Tokyo, 4-6-1 Shirokanedai, Minato-ku, Tokyo 108-8639, Japan. [2]Division of Molecular Therapy, Department of The advanced Clinical Research Center, The Institute of Medical Science, the University of Tokyo, 4-6-1 Shirokanedai, Minato-ku, Tokyo 108-8639, Japan. [3]Department of Blood Transfusion and Cellular Therapy, National Cancer Center Hospital, 5-1-1 Tsukiji, Chuo-ku, Tokyo 104-0045, Japan. [4]Department of Rare Diseases Research, Institute of Medical Science, St. Marianna University Graduate School of Medicine, Sugao, Miyamae-ku, Kawasaki, Kanagawa 216-8512, Japan.

Received: 15 August 2014 Accepted: 22 September 2014
Published: 4 October 2014

References
de Oliveira MF, Vieira M, Primo J, Siqueira IC, Carvalho EM, Farre L, Fatal PL, Bittencourt AL (2010) Flower cells in patients with infective dermatitis associated with HTLV-1. J Clin Virol 48:288–290

Dungerwalla M, Osuji N, Waldman AD, Jehani FAI, Mehta A, Taylor R, Wotherspoon A, Cogill G, Matutes E (2005) Isolated central nervous system involvement in adult T-cell lymphoma/leukaemia. Br J Haematol 130:511–515

Hempel L, Körholz D, Nussbaum P, Bönig H, Burdach S, Zintl F (1997) High interleukin-10 serum levels are associated with fatal outcome in patients after bone marrow transplantation. Bone Marrow Transplant 20:365–368

Hinuma Y, Nagata K, Hanaoka M, Nakai M, Matsumoto T, Kinoshita K, Shirakawa S, Miyoshi I (1981) Adult T-cell leukemia: antigen in an ATL cell line and detection of antibodies to the antigen in human sera. Proc Natl Acad Sci U S A 78:6476–6480

Kamble RT, Chang CC, Sanchez S, Carrum G (2007) Central nervous system graft-versus-host disease: report of two cases and literature review. Bone Marrow Transplant 39:49–52

Kami M, Matsumura T, Tanaka Y, Mikami Y, Miyakoshi S, Ueyama J, Morinaga S, Mori S, Machida U, Kanda Y, Chiba S, Sakamaki H, Hirai H, Muto Y (2000) Serum levels of soluble interleukin-2 receptor after bone marrow transplantation: a true marker of acute graft-versus-host disease. Leuk Lymphoma 38:533–540

Kami M, Hamaki T, Miyakoshi S, Murashige N, Kanda Y, Tanosaki R, Takaue Y, Tanigushi S, Hirai H, Ozawa K, Kasai M (2003) Allogeneic haematopoietic stem cell transplantation for the treatment of adult T-cell leukaemia/lymphoma. Br J Haematol 120:304–309

Kitajima M, Korogi Y, Shigematsu Y, Murashige M, Kanda Y, Tanosaki R, Takaue Y, Taniguchi S, Hirai H, Ozawa K, Kasai M (2002) Central nervous system lesions in adult T-cell leukaemia: MRI and pathology. Neuroradiology 44:559–567

Maier LM, Anderson DE, Severson CA, Baecher-Allan C, Healy B, Liu DV, Wittrup KD, De Jager PL, Hafler D (2009) Soluble IL-2RA levels in multiple sclerosis subjects and the effect of soluble IL-2RA on immune responses. J Immunol 182:1541–1547

Mapara MY, Leng C, Kim YM, Bronson R, Loksbin A, Luster A, Sykes M (2006) Expression of chemokines in GVHD target organs is influenced by conditioning and genetic factors and amplified by GVHR. Biol Blood Marrow Transplant 12:623–634

Marshall AG, Pawson R, Thom M, Shuz TF, Scaravilli F, Rudge P (1998) HTLV-I associated primary CNS T-cell lymphoma. J Neurol Sci 158:226–231

Matsumoto M, Sugimoto M, Nakashima H, Imamura F, Kawano O, Uyama E, Takatsu K, Araki S (1990) Spontaneous T cell proliferation and release of

soluble interleukin-2 receptors in patients with HTLV-I-associated myelopathy. Am J Trop Med Hyg 42:365–373

McGill NK, Vyas J, Shimauchi T, Tokura Y, Piguet V (2012) HTLV-1-associated infective dermatitis: updates on the pathogenesis. Exp Dermatol 21:815–821

Misu T, Onodera H, Fujihara K, Matsushima K, Yoshie O, Okita N, Takase S, Itoyama Y (2001) Chemokine receptor expression on T cells in blood and cerebrospinal fluid at relapse and remission of multiple sclerosis: imbalance of Th1/Th2-associated chemokine signaling. J Neuroimmunol 114:207–212

Mitsuhiro O (1990) Review of WHO kagoshima meeting and diagnostic guidelines for HAM/TSP. Raven Press, New York, pp 191–197

Mochizuki M, Watanabe T, Yamaguchi K, Yoshimura K, Nakashima S, Shirao M, Araki S, Takatsuki K, Mori S, Miyata N (1992) Uveitis associated with human T-cell lymphotropic virus type I. Am J Ophthalmol 114:123–129

Natsumi A, Tomoo S, Hitoshi A, Yoshihisa Y (2014) HTLV-1 induces a Th1-like state in CD4+CCR4+ T cells. J Clin Invest 124:3431–3442

Niederwieser D, Huber C, Gratwohl A, Bannert P, Fuchs D, Hausen A, Reibnegger D, Speck B, Wachter H (1984) Neopterin as a new biochemical marker in the clinical monitoring of bone marrow transplant recipients. Transplantation 38:497–500

Ohba N, Matsumoto M, Sameshima M, Kabayama Y, Nakao K, Unoki K, Uehara F, Kawano K, Maruyama I, Osame M (1989) Ocular manifestations in patients infected with human T-lymphotropic virus type I. Jpn J Ophthalmol 33:1–12

Osame M, Usuku K, Izumo S, Ijichi N, Amitani H, Igata A, Matsumoto M, Tara M (1986) HTLV-I associated myelopathy, a new clinical entity. Lancet 1:1031–1032

Poiesz BJ, Ruscetti FW, Gazdar AF, Bunn PA, Minna JD, Gallo RC (1980) Detection and isolation of type C retrovirus particles from fresh and cultured lymphocytes of a patient with cutaneous T-cell lymphoma. Proc Natl Acad Sci U S A 77:7415–7419

Sato T, Coler-Reilly A, Utsunomiya A, Araya N, Yagishita N, Ando H, Yamauchi J, Inoue E, Ueno T, Hasegawa Y, Nishioka K, Nagajima T, Jacobson S, Izumo S, Yamano Y (2013) CSF CXCL10, CXCL9, and neopterin as candidate prognostic biomarkers for HTLV-1-associated myelopathy/tropical spastic paraparesis. PLoS Negl Trop Dis 7:e2479

Shimoyama M, Ota K, Kikuchi M, Yunoki K, Konda S, Takatsuki K, Ichimaru M, Tominaga S, Tsugane S, Minato K, Tobinai K, Oyama A, Hisano S, Matsumoto M, Takiguchi T, Yamaguchi K, Kinoshita K, Tajima K, Suemasu K (1988) Major prognostic factors of adult patients with advanced T-cell lymphoma/leukemia. J Clin Oncol 6:1088–1097

Tsukasaki K, Utsunomiya A, Fukuda H, Shibata T, Fukushima T, Takatsuka Y, Ikeda S, Masuda M, Nagoshi H, Ueda R, Tamura K, Sano M, Momita S, Yamaguchi K, Kawano F, Hanada S, Tobinai K, Shimoyama M, Hotta T, Tomonaga M (2007) VCAP-AMP-VECP compared with biweekly CHOP for adult T-cell leukemia-lymphoma: Japan Clinical Oncology Group Study JCOG9801. J Clin Oncol 25:5458–5464

Tsukasaki K, Hermine O, Bazarbachi A, Ratner L, Ramos JC, Harrington W, Jr, O'Mahony D, Janik JE, Bittencourt AL, Taylor GP, Yamaguchi K, Utsunomiya A, Tobinai K, Watanabe T (2009) Definition, prognostic factors, treatment, and response criteria of adult T-cell leukemia-lymphoma: a proposal from an international consensus meeting. J Clin Oncol 27:453–459

Uchiyama T, Yodoi J, Sagawa K, Takatsuki K, Uchino H (1977) Adult T-cell leukemia: clinical and hematologic features of 16 cases. Blood 50:481–492

Utsunomiya A, Miyazaki Y, Takatsuka Y, Hanada S, Uozumi K, Yashiki S, Tara M, Kawano F, Saburi Y, Kikuchi H, Hara M, Sao H, Morishima Y, Kodera Y, Sonoda S, Tomonaga M (2001) Improved outcome of adult T cell leukemia/lymphoma with allogeneic hematopoietic stem cell transplantation. Bone Marrow Transplant 27:15–20

doi:10.1186/2193-1801-3-581
Cite this article as: Kawamata *et al.*: A case of post-transplant adult T-cell leukemia/lymphoma presenting myelopathy similar to but distinct from human T-cell leukemia virus type I (HTLV- I)-associated myelopathy. *SpringerPlus* 2014 **3**:581.

Tomohiro Ishigaki*, Yuji Zaike, Masanori Nojima, Seiichiro Kobayashi, Nobuhiro Ohno, Kaoru Uchimaru, Arinobu Tojo, Hiromitsu Nakauchi and Nobukazu Watanabe

Quantification of adult T-cell leukemia/lymphoma cells using simple four-color flow cytometry

Abstract

Background: The absolute number of adult T-cell leukemia/lymphoma (ATL) cells in peripheral blood is an essential indicator to evaluate disease status. However, microscopically counting ATL cells based on morphology requires experience and tends to be inaccurate due to the rarity of ATL.

Methods: Based on our research showing that acute-type ATL cells are specifically enriched in the CD4+/CD7- (CD7N) fraction, a new analytical method to accurately quantify ATL cells was established using an internal bead standard and simple four-color flow cytometry. This method was verified by comparison with microscopic examination of 49 peripheral blood samples and used to follow up patients.

Results: A strong correlation was observed between the number of CD7N cells measured by flow cytometry and the number of abnormal lymphocytes measured microscopically by experienced technicians [Pearson's R, 0.963; Spearman's rho, 0.921; intercorrelation coefficient, 0.962]. The linear regression coefficient was close to 1 (β=1.013). Our method could detect 1 cell/μL, and the limit of quantitation was between 2.9 and 9.8 cells/μL. The frequency of CD7N cells among CD4+ cells changed during chemotherapy, which reflected differences between chemosensitive and chemoresistant cases. Kaplan-Meier analysis with a log-rank test showed that patients with decreased CD7N proportion after chemotherapy had significantly longer disease-specific survival (p=0.003).

Conclusions: Our newly established method quantified tumor cells in patients with acute-type ATL. Furthermore, this method was useful for assessing the efficacy of chemotherapy, and the change of the CD7N proportion could be more important to predict prognosis.

Keywords: adult T-cell leukemia/lymphoma (ATL); flow cytometry; HAS-Flow; human T-cell leukemia virus type 1 (HTLV-1).

DOI 10.1515/cclm-2014-0183
Received February 19, 2014; accepted June 18, 2014

***Corresponding author: Tomohiro Ishigaki,** Clinical FACS Core Laboratory, Institute of Medical Science, University of Tokyo, 4-6-1 Shirokanedai, Minato-ku, Tokyo 108-8639, Japan, Phone: +81 3 5449 5765, Fax: +81 3 5449 5750, E-mail: ishigaki@ims.u-tokyo.ac.jp; and Institute of Medical Science, Division of Stem Cell Therapy, University of Tokyo, Tokyo, Japan
Yuji Zaike: Institute of Medical Science, Department of Laboratory Medicine, Research Hospital, University of Tokyo, Tokyo, Japan
Masanori Nojima: Institute of Medical Science, Division of Advanced Medicine Promotion, University of Tokyo, Tokyo, Japan
Seiichiro Kobayashi: Institute of Medical Science, Division of Molecular Therapy, University of Tokyo, Tokyo, Japan
Nobuhiro Ohno and Kaoru Uchimaru: Institute of Medical Science, Department of Hematology and Oncology, Research Hospital, University of Tokyo, Tokyo, Japan
Arinobu Tojo: Institute of Medical Science, Division of Molecular Therapy, University of Tokyo, Tokyo, Japan; and Institute of Medical Science, Department of Hematology and Oncology, Research Hospital, University of Tokyo, Tokyo, Japan
Hiromitsu Nakauchi: Institute of Medical Science, Division of Stem Cell Therapy, University of Tokyo, Tokyo, Japan
Nobukazu Watanabe: Clinical FACS Core Laboratory, Institute of Medical Science, University of Tokyo, Tokyo, Japan

Introduction

Adult T-cell leukemia/lymphoma (ATL) is a mature T-cell neoplasm caused by human T-cell leukemia virus type 1 (HTLV-1). According to the classification of the Japanese Lymphoma Study Group (Shimoyama classification) [1], ATL is classified into four subtypes: smoldering, chronic, lymphoma, and acute-type. Chemotherapy should be offered to patients with acute, lymphoma, and chronic-type ATL with unfavorable prognostic factors.

A quantitative analysis of ATL cells is essential to evaluate the therapeutic effect. The number of ATL cells is currently estimated based on morphological abnormalities. Cells with abnormally hyperlobulated nuclei, which are termed 'flower cells', are characteristic ATL cells, but ATL cells are not always typical flower cells. ATL cells are morphologically diverse among cases, and the histological feature of ATL is diffuse proliferation of abnormal cells that vary in size and shape [2]. As discriminating ATL cells

morphologically from other lymphocytes, particularly from reactive atypical lymphocytes, is difficult, experience is required. Consequently, these difficulties cause differences between examiners and errors; therefore, morphological quantification of ATL cells tends to be inaccurate.

Many researchers have attempted to develop other counting methods or to identify markers that reflect the number of ATL cells [3–9]. The most prevalent method is HTLV-1 proviral load (PVL), measured by quantitative real-time polymerase chain reaction [5–9]. Although PVL in peripheral blood mononuclear cells (PBMCs) is a surrogate marker of the number of HTLV-1-infected cells, it has several problems. First, PVL can be affected by the total number of PBMCs, as it is only expressed as a percentage in PBMCs and not an absolute value. Second, PVL reflects only the burden of infection and is not specific for ATL cells. Third, PVL may overestimate the frequency of ATL cells when ATL cells harbor multiple copies within a single cell [5]. Furthermore, PVL measurements vary widely among laboratories, and should be standardized [10]. Finally, the method is time-consuming and is not sufficiently easy to use frequently for clinical testing. Therefore, establishing a new method to quantify ATL cells more accurately and easily is required.

We assessed a number of samples from patients with ATL using 12-color flow cytometry, and have established the flow cytometric method named 'HAS (HTLV-1 Analyzing System)-Flow,' to analyze ATL cells. Downregulation of CD3 and CD7 is observed in ATL cells, and we reported that CD4-positive cells in patients with ATL can be classified into three groups of: $CD3^{positive}/CD7^{positive}$ (CD7P), $CD3^{dimly\ positive}/CD7^{dimly\ positive}$ (CD7D), and $CD3^{dimly\ positive}/CD7^{negative}$ (CD7N) [11]. Examining the PVL showed that HTLV1-infected cells were concentrated mainly in the CD7N fraction in patients with acute-type ATL. Moreover, the Vβ repertoire revealed that tumor cells are specifically enriched in the CD7N fraction, usually to almost 100% after assessing clonality in the context of the T-cell receptor [11]. Therefore, the number of CD7N cells reflects the number of ATL cells. We applied these findings to a new clinical test, and established a new analytical method using simple four-color flow cytometry.

Materials and methods

Patient samples

Peripheral blood samples were collected from patients with acute-type ATL who were admitted to the Research Hospital at the Institute of Medical Science, University of Tokyo (IMSUT) between June 2011 and December 2012. Some of the patients were transferred to our hospital after a few courses of chemotherapy. This study was approved by the Research Ethics Committee of IMSUT, and written informed consent was obtained from all patients in accordance with the Declaration of Helsinki. All patients were diagnosed with acute-type ATL according to Shimoyama's criteria [1] and had not received hematopoietic stem cell transplantation (HSCT). In total, 49 samples from 14 patients were collected before treatment or just before a course of chemotherapy (Table 1). The effectiveness of chemotherapy was evaluated using the ATL response criteria [12].

Sample preparation and immunofluorescence staining

Peripheral blood was obtained in Vacutainer Hemogard Plus tubes (BD Biosciences, San Jose, CA, USA) by conventional venipuncture. As the volume required for our method was only 100 µL, the rest of peripheral blood samples used for routine laboratory tests were applied for measurement. A ProCOUNT method using Trucount tubes (BD Biosciences), in which a known number of fluorescent reference beads are included, was adopted to measure the absolute number of cells. First, fluorescently labeled antibodies, consisting of fluorescein isothiocyanate (FITC)-CD4 (BioLegend, San Diego, CA, USA), phycoerythrin (PE)-CD7 (BD Pharmingen, San Jose, CA, USA), allophycocyanin (APC)-CD3 (BioLegend), and PerCP-Cy5.5-CD14 (BioLegend), were mixed in a Trucount tube. Then, 100 µL of whole peripheral blood were added to the tube and mixed well. The cells were stained for 15 min at room temperature. After staining, 1 mL of Cell Lysis Buffer (BD Biosciences) was added to lyse the red blood cells. After 15 min, the sample was vortexed gently for 10 s and analyzed with a FACSCalibur flow cytometer (BD Immunocytometry Systems, San Jose, CA, USA) as soon as possible.

Sorting, cytospin, and Wright-Giemsa staining

A FACS Aria II SORP flow cytometer (BD Immunocytometry Systems) was used for cell sorting. Sorted cells were fixed on glass slides by cytospinning (20×g, 5 min) and subjected to Wright-Giemsa staining.

Flow cytometric analysis

Flow cytometry data were analyzed with FlowJo 9.6 (Treestar, San Carlos, CA, USA). We defined CD4-positive cells according to the gating procedure shown in Figure 1. The first gate on the FSC versus SSC plot was set relatively wide so as not to miss lymphocytes (Figure 1A), because adjacent monocytes and hemolytic debris could be excluded by subsequent CD14-negative selection (Figure 1B) and CD4-positive selection steps (Figure 1C). Purified CD4-positive cells were drawn in a pseudo-color plot (Figure 1E) and in a contour plot (Figure 1F). The borders among CD7P, CD7D, and CD7N in the CD7 versus CD3 plot were drawn according to contour lines (Figure 1F). Reference beads were gated in the PE versus FITC plot, according to the manufacturer's instructions (Figure 1D).

Table 1 Forty-nine samples from 14 patients with acute-type ATL were analyzed.

Patient ID	Age	Sex	Number of analysis	Average interval of analysis (range)	At the first flow cytometric evaluation					CD3 expression of ATL cells	HSCT before/during analysis
					CD7P, /μL	CD7D, /μL	CD7N, /μL	WBC, /μL	Normal lymphocytes, %	Abnormal lymphocytes, %	
1	62	M	2	14	12.9	36.4	538.0	2340	7.0	38.0	Dim	-
2	38	F	3	38.5 (14–63)	247.8	92.9	15,144.9	25,020	5.7	71.2	Dim	-
3	43	M	4	28.0 (13–43)	81.1	173.6	200.9	10,790	7.4	2.4	Dim	-
4	69	M	4	25.0 (14–40)	63.4	60.7	116.9	3450	7.5	3.0	Dim	-
5	62	M	4	17.7 (14–20)	68.0	172.7	838.5	11,310	8.5	8.5	Dim	-
6	62	M	2	27	907.7	5214.6	13,191.0	27,230	8.4	65.4	Dim	-
7	63	F	7	44.5 (30–57)	116.2	26.8	544.6	3620	12.4	21.4	Dim	-
8	67	M	6	36.2 (12–53)	189.5	266.4	290.3	10,280	15.3	3.8	Dim	-
9	50	M	6	30.0 (14–54)	86.3	112.9	6442.3	19,050	3.3	33.0	Dim	-
10	50	M	1	-	21.7	52.8	142.7	3800	10.3	3.0	Dim	-
11	44	M	1	-	683.8	184.4	6815.1	22,840	11.0	33.0	Negative	-
12	59	M	3	27.5 (27–28)	312.9	480.3	1951.4	7550	16.0	38.0	Dim	-
13	72	M	4	28.0 (25–32)	129.6	28.9	397.8	11,520	4.0	5.5	Dim	-
14	63	M	2	29	167.1	164.0	115.7	4590	23.5	1.0	Dim	-

HSCT, hematopoietic stem cell transplantation

The absolute number of cells was accurately calculated from the ratio of beads to cells in the region of the interest (Figure 1G). For example, when the total number of beads in a Trucount tube was 52187, the number of CD7N cells in the case in Figure 1 was calculated as follows: CD7N cells=(5482/100)×(52187/5201)=550.1/μL.

Validation of the flow cytometric quantification

Cryopreserved PBMCs of acute-type ATL patients were used for validation of this assay, and CD4+CD7N cells were quantified in the same way indicated above. As a blank control, phosphate buffered saline (PBS) was used. The intra-assay variation was assessed by calculating the coefficient of variation (CV) with 10 different density gradients ranging from 0 to 30000 cells/μL. Each sample was assayed six times. The limits of detection (LoD) and quantitation (LoQ) were also assessed. The LoQ was determined by the lowest concentration whose six replicates had a CV <20%. The inter-assay variation was assessed by calculating the CV of multiple determinations of a same sample measured on different days.

Conventional assessment of morphologically abnormal lymphocytes

When samples were examined by flow cytometry, total white blood cell (WBC) counts (normal range, 3500–9100/μL) were performed mechanically using an XE-2100 system (Sysmex, Kobe, Japan), and 300–400 WBCs per sample were classified by clinical technicians who were skilled in morphologically classifying ATL cells. Abnormal lymphocytes were classified according to the guideline of Japanese Association of Medical Technologists (JAMT). Briefly, lymphocytes with nuclear abnormalities, such as lobulated nuclei, multiple nuclei, evident nucleoli, or high nucleo-cytoplasmic ratio, were classified as abnormal lymphocytes. The absolute number of morphologically abnormal lymphocytes was calculated by multiplying their percentage by the total number of WBCs.

Measurement of LDH and sIL-2R

Disease status was also followed by lactate dehydrogenase (LDH) and soluble IL-2 receptor (sIL-2R). LDH activities were measured by the lactate-to-pyruvate assay according to the recommendations of the Japanese Society of Clinical Chemistry (normal range, 106–211 IU/L). Serum sIL-2R levels were measured by ELISA (normal range, 145–519 U/mL).

Statistical analysis

The correlation between the number of CD7N cells measured by flow cytometry and the number of abnormal lymphocytes measured by microscopic counting was assessed by Pearson's correlation coefficients (R), Spearman's correlation coefficients (rho), intra-class correlation coefficients (ICC), and linear regression coefficients.

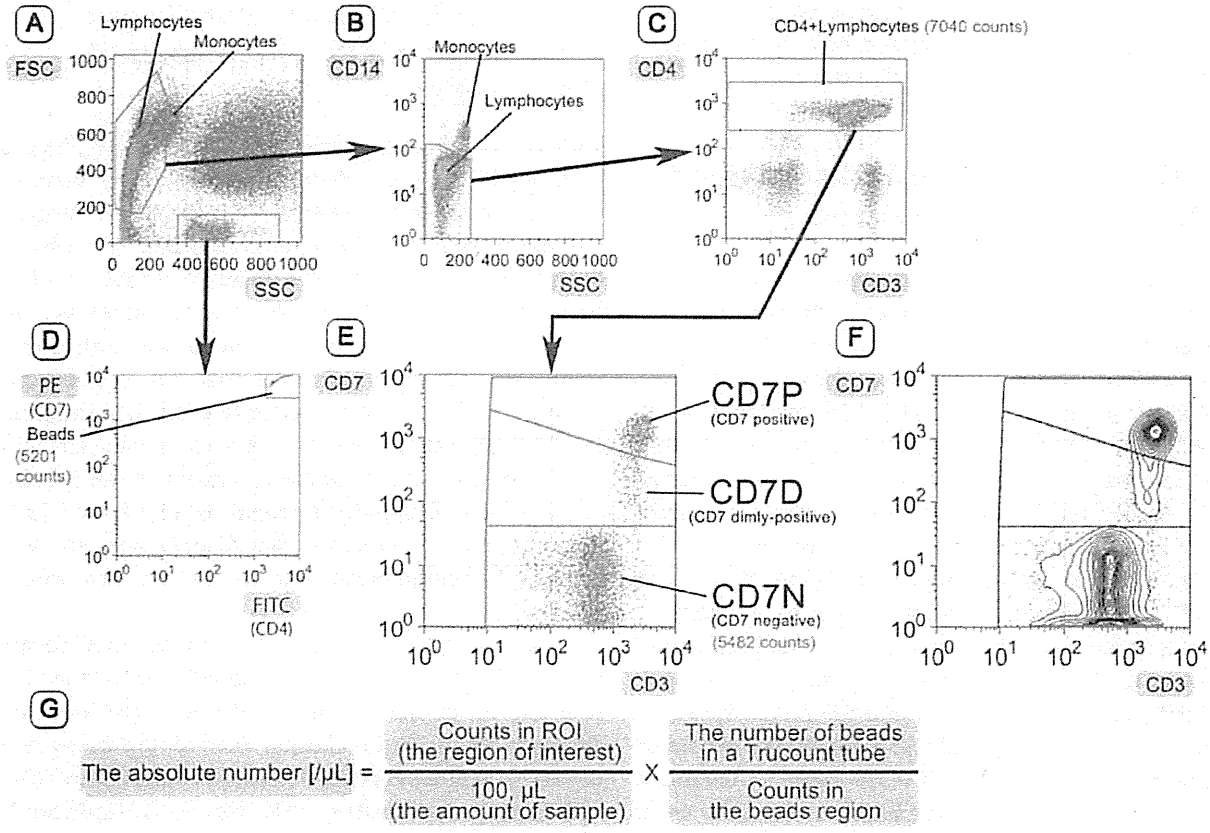

Figure 1 Flow cytometric gating procedure.
CD4-positive cells were properly defined according to the procedure shown here (A–C). CD4-positive cells were classified into CD7P, CD7D, and CD7N cells according to the contour lines of a CD7 versus CD3 plot (E, F). Reference beads were gated in the PE versus FITC plot (D). The absolute number of CD7N cells was calculated using this formula (G).

As data from both measurements followed a log-normal distribution, these analyses were performed after log-transformation. Bland-Altman analysis was used to calculate the agreement between flow cytometric and microscopic counting. In addition, the inverse probability weighting (IPW) method and mixed model (varying intercepts and slopes) were used due to the imbalance in sample number and individual differences between the patients. Kaplan-Meier analysis with a post hoc log-rank test was performed for disease-specific survival stratified by whether relative decrease of the CD7N proportion after the chemotherapy was over 5% or not. Statistical analyses were performed using the GraphPad Prism software, ver. 6.0c (GraphPad Software Inc., San Diego, CA, USA) and SPSS software ver. 20 (IBM Corp., Armonk, NY, USA).

Results

Abnormal lymphocytes are enriched in the CD7N fraction

Along with our previous research using 12-color flow cytometry, simple four-color flow cytometry could classify CD4-positive lymphocytes into three groups of: CD7P, CD7D, and CD7N (Figure 1). Almost all of CD7-negative cells were dimly-positive for CD3, except for a case in which CD7-negative cells were all negative for CD3. In the representative case of acute-type ATL where the proportions of CD7P, CD7D, and CD7N in CD4+ cells were 2.7%, 1.7%, and 95.6%, the proportions of abnormal lymphocytes in these three fractions were 0.0%, 6.0%, and 99.0%, respectively. Morphological evaluation showed that almost all CD7N cells were morphological abnormal, whereas none of the CD7P cells were abnormal.

Intra- and inter-assay variation of this flow cytometric quantification was low

To evaluate the precision of our assay, we assessed the intra-assay CVs of 10 different density gradients. The intra-assay CVs of samples with the average of 1.2, 2.9, 9.8, 20.5, 42.7, 442.7, 1073.7, 8081.2, and 30,729.8 cells/μL were 30.69, 31.17, 5.94, 4.89, 3.64, 4.02, 4.61, 2.45, and 4.98%, respectively. Six determinations of a blank control were all measured to be

0 cells/μL. The limit of detection was about 1 cell/μL, and the limit of quantitation was estimated to be between 2.9 and 9.8 cells/μL. The inter-assay CV was 5.81%.

Correlation between CD7N cells and morphologically abnormal lymphocytes

We found a significant correlation between the number of CD7N cells and the number of morphologically abnormal lymphocytes (Pearson's R=0.963, Spearman's ρ=0.921, and ICC=0.962; Figure 2A). Moreover, the linear regression coefficient was close to 1 [β=1.013, 95% confidence interval (CI), 0.991–1.034]. The calculated number of CD7N cells was often similar to the number of morphologically abnormal lymphocytes. In two cases, flow cytometric analysis detected ATL cells but microscopic counting did not.

In addition, we reassessed the correlation using the IPW method and the mixed model considering the imbalance in sample number and individual differences between patients. Using the IPW method, Pearson's R=0.973, Spearman's ρ=0.942, and the linear regression coefficient was 1.010 (95% CI 0.990–1.030). The regression coefficient was 0.979 (95% CI 0.893–1.064) in the mixed model. Almost all results were improved from the crude analysis, and the influences of sampling imbalance and individual differences were limited.

The Bland-Altman plot showed good agreement between both measurements (Figure 2B). There seemed to be little additive or proportional bias.

The change in the CD7-CD3 profile was useful to evaluate the effectiveness of chemotherapy

We then compared the change in a CD7 versus CD3 plot of CD4-positive cells during chemotherapy between chemoresistant and chemosensitive cases. The proportion of CD7N cells in chemoresistant cases increased or did not change, although the absolute number of CD7N cells decreased slightly. In the case of Figure 3A, i.e., both the number of ATL cells and lactate dehydrogenase (LDH) decreased after the first course of chemotherapy, and the response seemed good. Nevertheless, the CD7-CD3 profile was almost unchanged. After the second course, all parameters, including the number of ATL cells and the LDH and soluble interleukin (IL)-2 receptor levels, increased. The disease was not controlled by chemotherapy, and the patient died after 1 month.

In contrast, the CD7-CD3 profile changed dramatically in clinically good responders who achieved a complete response or partial response. Representative data are shown in Figure 3B. In addition to an abrupt decrease in the absolute number of CD7N cells, the frequency of CD7N cells among CD4-positive cells decreased significantly, whereas the frequency of CD7P cells increased. While a significant proportion of patients with acute-type ATL cannot undergo HSCT because of uncontrollable disease, the patient in Figure 3B received allogeneic HSCT after several courses of chemotherapy.

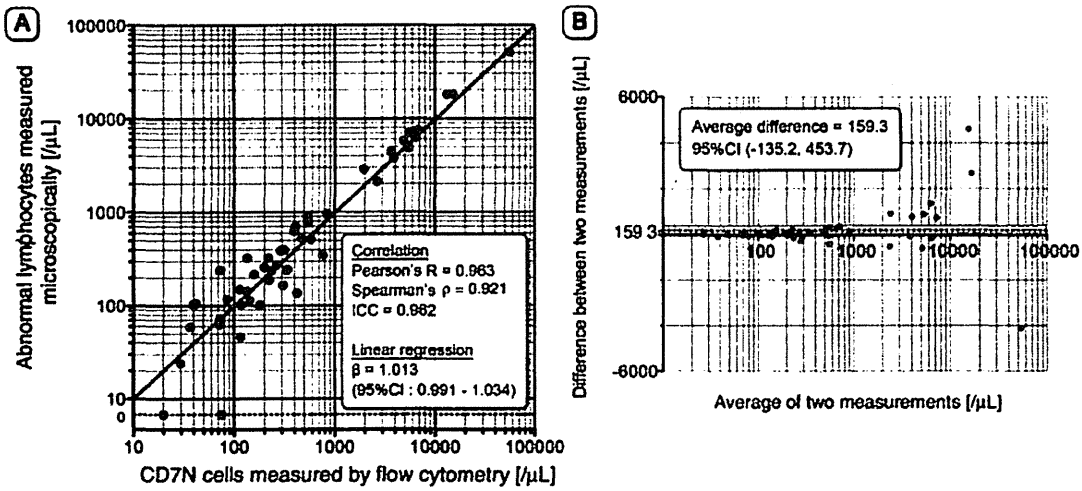

Figure 2 The correlation between CD7N cells and abnormal lymphocytes.
The correlation between CD7N cells measured by flow cytometry and abnormal lymphocytes measured microscopically was evaluated using three correlation tests and a linear regression analysis (A). The agreement between the two measurements was analyzed with a Bland-Altman plot (B).

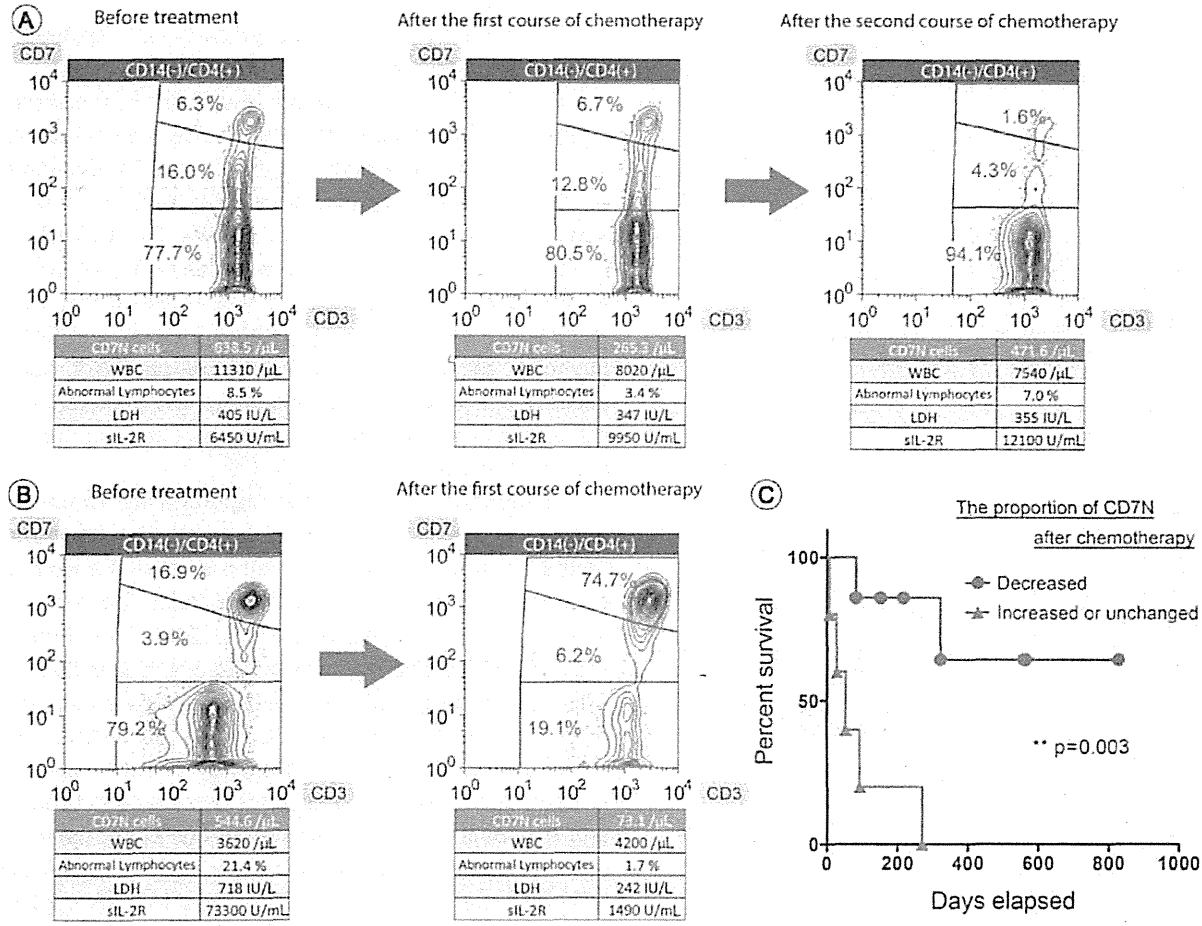

Figure 3 The CD7-CD3 profile allowed for an assessment of chemotherapy efficacy and could predict prognosis.
A patient with an almost unchanged CD7-CD3 profile after the first course of chemotherapy had an unfavorable prognosis after the second course (A). In contrast, a patient that showed a good clinical response to chemotherapy exhibited marked changes in the CD7-CD3 profile after only one course of chemotherapy (B). Kaplan-Meier suvival curves showed ATL patients with decreased CD7N proportion after chemotherapy showed significantly longer disease-specific survival (p=0.003) (C).

The pattern of change in the CD7-CD3 profile was observed repeatedly in many patients to reflect the effectiveness of chemotherapy, and these results suggested that the change in the CD7-CD3 profile is useful to assess the effect of chemotherapy.

ATL patients with decreased CD7N proportion after chemotherapy showed longer disease-specific survival

Next, we focused on the first chemotherapy during flow cytometric analyses periods, and examined the relation between the prognosis and the change of clinical parameters (Table 2). Consequently, the CD7N proportion was picked up, and acute-type ATL patients were classified into two groups by the relative change of the CD7N proportion after the chemotherapy. The CD7N proportion was considered decreased when a relative decrease of more than 5% was achieved after chemotherapy compared with the one before the chemotherapy. ATL patients with decreased CD7N proportion after chemotherapy showed longer survival than ones with unchanged or increased (Figure 3C). A log-rank test showed that there was a significant difference between the two groups (p=0.003). The difference suggested that the change in the CD7N proportion could be more important to predict the prognosis.

Discussion

Based on our previous studies [11, 13], we applied research findings to a clinical test. We made the procedure as simple as possible to maximize practicality after several

Table 2 The change of clinical parameters after the first chemotherapy.

Patient ID	Before chemotherapy				After chemotherapy				Change of CD7N proportion after chemotherapy	HSCT after flow cytometric analysis	Outcome (days after post-chemotherapy evaluation)
	Proportion of CD7N, %	Absolute number of CD7N, /μL	LDH, IU/L	sIL-2R, U/mL	Proportion of CD7N,%	Absolute number of CD7N, /μL	LDH, IU/L	sIL-2R, U/mL			
1	91.6	538.0	774	22,600	96.1	115.2	651	–	Increased	–	Died of ATL (7)
2	97.8	15,144.9	272	24,100	97.4	5479.9	108	27,700	Unchanged	–	Died of ATL (93)
3	44.1	200.9	376	4200	37.6	72.8	273	7420	Decreased	+	Died of ATL (322)
4	48.5	116.9	446	4040	60.7	181.2	717	22,200	Increased	–	Died of ATL (28)
5	77.7	838.5	405	6450	80.5	265.3	347	9950	Increased	–	Died of ATL (54)
6	68.3	13,191.0	633	11,700	57.9	2640.0	283	3500	Decreased	+	Died of ATL (83)
7	79.2	544.6	718	73,300	19.1	73.1	242	1490	Decreased	+	Alive in CR (828)
8	38.9	290.3	259	3500	30.9	796.5	200	2300	Decreased	–	Died of infection (152)[a]
9	97.0	6442.3	655	17,200	96.2	3859.2	392	21,400	Unchanged	+	Died of ATL (270)
12	71.1	1951.4	582	15,500	65.2	577.1	238	2840	Decreased	+	Alive in CR (565)
13	71.5	397.8	251	6340	59.6	335.6	169	1420	Decreased	–	Alive in CR (559)
14	25.9	115.7	293	5230	14.3	29.7	452	7820	Decreased	–	Transferred to another hospital (217)[a]

[a]ATL was under control when patients were censored.

trials, and finally established a practical flow cytometry method to quantify acute-type ATL cells.

Flow cytometry is highly sensitive in detecting minimal residual disease (MRD) of hematological malignancies. Similar flow cytometric approach for detection of MRD in ATL was reported previously, and a multi-parametric approach using CD2, CD3, CD4, CD5, CD7, CD25, CD26, and CD27 was useful for detection of ATL cells [14]. We established here a more practical and easier flow cytometric method using only CD3, CD4, CD7, and CD14. Moreover we limited the use to acute-type ATL cases because our previous studies showed the expression of cell surface antigens on ATL cells was slightly different among subtypes.

Combination of gates is also important and characteristic of our method. We showed here all the procedures including gating and quantification so that the method could be easily applied in other hospitals. This test provides accurate quantification of CD7N lymphocytes achieved by establishing an appropriate gating procedure (Figure 1). As a first gate, two methods are generally used to gate lymphocytes. One is FSC versus SSC gating, and the other is CD45 versus SSC gating [15]. The latter method is often used to analyze malignant hematologic diseases and eliminate red blood cell debris but is not convenient to analyze ATL cells because these occasionally lose [16] or express a high level of CD45. Therefore, we applied FSC versus SSC gating for lymphocyte gating. Moreover, eliminating monocytes is necessary to precisely enumerate CD7N lymphocytes because monocytes are weakly positive for CD4 and negative for CD7. Hence, we gated out monocytes carefully by CD14 staining before CD4-positive selection. Combination of the first wide lymphocyte gate and the following two strict gates enabled purification of CD4-positive lymphocytes without excess or deficiency. Then, CD7N cells were defined according to the contour lines in a plot of CD4-positive lymphocytes. Drawing the border between CD7D and CD7N cells was easy because contour lines clearly and horizontally separated these two populations. In contrast, the border between CD7P and CD7D cells was sometimes difficult to determine; thus, further improvement may be needed. However, the latter border is not necessary to estimate the number of ATL cells using this method.

Although the number of ATL cells is currently estimated based on morphologically abnormal cells, morphological evaluation of ATL cells often differs between examiners. Particularly, morphological enumeration by inexperienced examiners tends to be inaccurate. We therefore assessed here the correlation between the number of CD7N cells and the number of morphologically

abnormal lymphocytes evaluated only by experienced technicians (Figure 2A). As expected, a strong correlation was identified. It is noteworthy that the regression coefficient was very close to 1.0. This new flow cytometric method is useful for accurate evaluation of ATL cells. Furthermore, only flow cytometry detected ATL cells in two cases. As the validation study of the assay showed very low limits of detection and quantitation, flow cytometry could detect ATL cells more sensitively than microscopic counting.

The Bland-Altman plot also showed good agreement and the relatively small average difference between the two measurements (Figure 2B). However, the three samples with the highest WBCs had high differences between the two methods. While flow cytometry allows rapid and accurate analysis of a much larger number of cells, manual counting has limitations in accuracy and the number of counts. Since the absolute number of morphologically abnormal lymphocytes was calculated by multiplying their percentage by the total number of WBCs, the margin of error in microscopic counting tended to get larger as the number of WBCs got higher. Although the relative differences between the two methods were generally not so high, these findings suggested the number of abnormal lymphocytes in samples with high WBC counts should be carefully examined.

This flow cytometry-based method has many advantages compared to PVL. First, flow cytometry allows for calculation of the absolute number of ATL cells, which is not affected by the number of other cells. Second, intra- and inter-assay variations of our method were confirmed to be low. The inter- and intra-laboratory variabilities of the ProCOUNT method are also known to be low [17]. Therefore, this flow cytometric method is precise and can be easily standardized. Third, it is practical and takes no more than 1 h.

In addition to its usefulness for quantitation, we also found that the change in the CD7-CD3 profile discriminated cases sensitive to chemotherapy and may predict prognosis (Figure 3A and B). Serum sIL-2R and LDH levels are also clinically important [18, 19], but they are not as specific for disease status because they are influenced by other factors, such as infection, inflammation, and hemolysis. Patients with a better prognosis tended to have a markedly better change in the CD7-CD3 profile after only one course of chemotherapy. In contrast, cases with unchanged or worse CD7-CD3 profiles after one course of chemotherapy tended to have an unfavorable prognosis after the second course, even if the number of ATL cells decreased, or the levels of sIL-2R and LDH improved initially.

From various parameters of the CD7-CD3 profile, we had tried picking up prognostic indicators. We focused on the first chemotherapy, and examined the change of various clinical parameters (Table 2) and their relation with survival. Needless to say, the number of CD7N cells, as the number of ATL cells, was important to evaluate the disease status through the follow-up, and robust reduction of the number of CD7N cells was necessary for a better prognosis. However, the change of the CD7N proportion seemed more sensitive. We examined the relationship between the disease-specific survival and the relative change of the CD7N proportion after chemotherapy. Although the number of patients was limited, it is noteworthy that patients with decreased CD7N proportion had significantly longer survival (Figure 3C). Further accumulation of cases and longer follow-up are warranted to elucidate the ability of this method to predict prognosis.

Our experience suggests that this method can be applied to almost all patients with acute-type ATL. However, some limitations should be noted. First, this method did not accurately detect ATL cells in patients who had undergone HSCT, as downregulation of CD7 in CD4-positive non-ATL lymphocytes was observed in most cases [20]. Second, this method cannot identify ATL cells in rare cases in which ATL tumor cells lack CD4 expression or express CD7. Therefore, a brief confirmation of the ATL phenotype using other surface markers is recommended before flow cytometric quantification.

In summary, we established a clinical test to accurately quantify ATL cells in patients with acute-type ATL using simple four-color flow cytometry. This newly established clinical application of 'HAS-Flow' will provide more accurate enumeration of ATL cells and assessment of chemosensitivity.

Acknowledgments: We would like to thank Dr. Naoki Oyaizu and Dr. Naoyuki Isoo (Laboratory Medicine, Research Hospital, Institute of Medical science) for their kind permission to introduce this clinical test, as well as Mr. Yukihisa Tanaka, Ms. Etsuko Nagai, and Ms. Motoko Mizukami for their excellent morphological classification.
Author contributions: All the authors have accepted responsibility for the entire content of this submitted manuscript and approved submission.
Research funding: None declared.
Employment or leadership: None declared.
Honorarium: None declared.
Competing interests: The funding organization(s) played no role in the study design; in the collection, analysis, and interpretation of data; in the writing of the report; or in the decision to submit the report for publication.

References

1. Shimoyama M. Diagnostic criteria and classification of clinical subtypes of adult T-cell leukaemia-lymphoma. A report from the Lymphoma Study Group (1984–87). Br J Haematol 1991;79:428–37.
2. Ohshima K. Pathological features of diseases associated with human T-cell leukemia virus type I. Cancer Sci 2007;98:772–8.
3. de Souza JG, Fonseca FG, Martins-Filho OA, Teixeira-Carvalho A, Martins CP, Carvalho LD, et al. Diagnostic tool based on an HTLV-1-Tax expression system in eukaryotic cells using a poxvirus vector. J Virol Methods 2010;166:65–71.
4. Sadamori N. Clinical and biological significance of serum tumor markers in adult T-cell leukemia. Leuk Lymphoma 1996;22:415–9.
5. Kamihira S, Dateki N, Sugahara K, Hayashi T, Harasawa H, Minami S, et al. Significance of HTLV-1 proviral load quantification by real-time PCR as a surrogate marker for HTLV-1-infected cell count. Clin Lab Haematol 2003;25:111–7.
6. Waters A, Oliveira AL, Coughlan S, de Venecia C, Schor D, Leite AC, et al. Multiplex real-time PCR for the detection and quantitation of HTLV-1 and HTLV-2 proviral load: addressing the issue of indeterminate HTLV results. J Clin Virol 2011;52:38–44.
7. Moens B, Lopez G, Adaui V, Gonzalez E, Kerremans L, Clark D, et al. Development and validation of a multiplex real-time PCR assay for simultaneous genotyping and human T-lymphotropic virus type 1, 2, and 3 proviral load determination. J Clin Microbiol 2009;47:3682–91.
8. Takenouchi H, Umeki K, Sasaki D, Yamamoto I, Nomura H, Takajo I, et al. Defective human T-lymphotropic virus type 1 provirus in asymptomatic carriers. Int J Cancer 2011;128:1335–43.
9. Altamirano NA, Rocco C, Aulicino P, Sen L, Mangano A. Quantitation of HTLV-I proviral load by a real-time PCR assay using SYBR Green: comparison of two methods for DNA isolation. J Virol Methods 2010;170:160–4.
10. Kamihira S, Yamano Y, Iwanaga M, Sasaki D, Satake M, Okayama A, et al. Intra- and inter-laboratory variability in human T-cell leukemia virus type-1 proviral load quantification using real-time polymerase chain reaction assays: a multi-center study. Cancer Sci 2010;101:2361–7.
11. Tian Y, Kobayashi S, Ohno N, Isobe M, Tsuda M, Zaike Y, et al. Leukemic T cells are specifically enriched in a unique CD3(dim) CD7(low) subpopulation of CD4(+) T cells in acute-type adult T-cell leukemia. Cancer Sci 2011;102:569–77.
12. Tsukasaki K, Hermine O, Bazarbachi A, Ratner L, Ramos JC, Harrington W Jr., et al. Definition, prognostic factors, treatment, and response criteria of adult T-cell leukemia-lymphoma: a proposal from an international consensus meeting. J Clin Oncol 2009;27:453–9.
13. Kobayashi S, Tian Y, Ohno N, Yuji K, Ishigaki T, Isobe M, et al. The CD3 versus CD7 plot in multicolor flow cytometry reflects progression of disease stage in patients infected with HTLV-I. PLoS One 2013;8:e53728.
14. Shao H, Yuan CM, Xi L, Raffeld M, Morris JC, Janik JE, et al. Minimal residual disease detection by flow cytometry in adult T-cell leukemia/lymphoma. Am J Clin Pathol 2010;133:592–601.
15. Borowitz MJ, Guenther KL, Shults KE, Stelzer GT. Immunophenotyping of acute leukemia by flow cytometric analysis. Use of CD45 and right-angle light scatter to gate on leukemic blasts in three-color analysis. Am J Clin Pathol 1993;100:534–40.
16. Weil R, Levraud JP, Dodon MD, Bessia C, Hazan U, Kourilsky P, et al. Altered expression of tyrosine kinases of the Src and Syk families in human T-cell leukemia virus type 1-infected T-cell lines. J Virol 1999;73:3709–17.
17. Schnizlein-Bick CT, Spritzler J, Wilkening CL, Nicholson JK, O'Gorman MR. Evaluation of TruCount absolute-count tubes for determining CD4 and CD8 cell numbers in human immunodeficiency virus-positive adults. Site Investigators and The NIAID DAIDS New Technologies Evaluation Group. Clin Diagn Lab Immunol 2000;7:336–43.
18. Motoi T, Uchiyama T, Uchino H, Ueda R, Araki K. Serum soluble interleukin-2 receptor levels in patients with adult T-cell leukemia and human T-cell leukemia/lymphoma virus type-I seropositive healthy carriers. Jpn J Cancer Res 1988;79:593–9.
19. Araki K, Harada K, Nakamoto K, Shiroma M, Miyakuni T. Clinical significance of serum soluble IL-2R levels in patients with adult T cell leukaemia (ATL) and HTLV-1 carriers. Clin Exp Immunol 2000;119:259–63.
20. Leblond V, Othman TB, Blanc C, Theodorou I, Choquet S, Sutton L, et al. Expansion of CD4+CD7- T cells, a memory subset with preferential interleukin-4 production, after bone marrow transplantation. Transplantation 1997;64:1453–9.

Supplemental Material: The online version of this article (DOI: 10.1515/cclm-2014-0183) offers supplementary material, available to authorized users.

Cancer Science
Japanese Cancer Association JCA
Open Access

Epigenetic deregulation of *Ellis Van Creveld* confers robust Hedgehog signaling in adult T-cell leukemia

Ryutaro Takahashi,[1,6] Makoto Yamagishi,[1,6] Kazumi Nakano,[1] Toshiko Yamochi,[2] Tadanori Yamochi,[1] Dai Fujikawa,[1] Makoto Nakashima,[1] Yuetsu Tanaka,[3] Kaoru Uchimaru,[4] Atae Utsunomiya[5] and Toshiki Watanabe[1]

[1]Graduate School of Frontier Sciences, The University of Tokyo, Tokyo; [2]Department of Pathology, Showa University School of Medicine, Tokyo; [3]Department of Immunology, Graduate School of Medicine, University of the Ryukyus, Okinawa; [4]Institute of Medical Science, The University of Tokyo, Tokyo; [5]Department of Hematology, Imamura Bun-in Hospital, Kagoshima, Japan

Key words

ATL, epigenetics, EVC, Hedgehog, HTLV-1

Correspondence

Toshiki Watanabe, Laboratory of Tumor Cell Biology, Department of Medical Genome Sciences, Graduate School of Frontier Sciences, The University of Tokyo, 4-6-1 Shirokanedai, Minato-ku, Tokyo 108-8639, Japan.
Tel: +81-3-5449-5298; Fax: +81-3-5449-5418;
E-mail: tnabe@ims.u-tokyo.ac.jp

[6]These authors contributed equally to this study.

Funding information

JSPS KAKENHI (24790436). (23390250). MEXT KAKENHI (221S0001). Ministry of Health, Labour and Welfare H24-Third Term Cancer-004 Uehara Memorial Foundation.

Received April 14, 2014; Revised June 20, 2014; Accepted July 1, 2014

Cancer Sci **105** (2014) 1160–1169

doi: 10.1111/cas.12480

One of the hallmarks of cancer, global gene expression alteration, is closely associated with the development and malignant characteristics associated with adult T-cell leukemia (ATL) as well as other cancers. Here, we show that aberrant overexpression of the *Ellis Van Creveld* (EVC) family is responsible for cellular Hedgehog (HH) activation, which provides the pro-survival ability of ATL cells. Using microarray, quantitative RT-PCR and immunohistochemistry we have demonstrated that EVC is significantly upregulated in ATL and human T-cell leukemia virus type I (HTLV-1)-infected cells. Epigenetic marks, including histone H3 acetylation and Lys4 trimethylation, are specifically accumulated at the *EVC* locus in ATL samples. The HTLV-1 Tax participates in the coordination of EVC expression in an epigenetic fashion. The treatment of shRNA targeting EVC, as well as the transcription factors for HH signaling, diminishes the HH activation and leads to apoptotic death in ATL cell lines. We also showed that a HH signaling inhibitor, GANT61, induces strong apoptosis in the established ATL cell lines and patient-derived primary ATL cells. Therefore, our data indicate that HH activation is involved in the regulation of leukemic cell survival. The epigenetically deregulated EVC appears to play an important role for HH activation. The possible use of EVC as a specific cell marker and a novel drug target for HTLV-1-infected T-cells is implicated by these findings. The HH inhibitors are suggested as drug candidates for ATL therapy. Our findings also suggest chromatin rearrangement associated with active histone markers in ATL.

Adult T-cell leukemia (ATL) is a malignant T-cell disorder caused by infection with a human retrovirus, human T-cell leukemia virus type I (HTLV-1).[1–3] The prognosis of aggressive types of ATL is poor.[4] At present, ATL is an intractable disease in human beings. To prevent the development of ATL and the poor prognosis that is associated with it, the development of effective therapies based on the molecular characteristics is needed.

To explore effective drugs, precise understanding of the molecular mechanism of ATL pathogenesis is essential. We have previously reported that genetic and epigenetic imbalances and following aberrant gene expressions are the main framework for ATL tumor cells.[5,6] In addition, the involvement of systemic downregulation of cellular microRNA has been implicated in the leukemogenesis of ATL. So far, several host cellular signaling abnormalities induced by HTLV-1 Tax in the early phase of infection[6–8] and the aberrant activation of nuclear factor-kappa B (NF-κB) contribute to ATL leukemogenesis.[9,10] Although other several molecular deregulations have been suggested in ATL, we have not completely covered the landscape of signaling networks in ATL.

Recently, Hedgehog (HH) signaling has been reported as an oncogenic pathway in many types of cancers.[11,12] Constitutive HH activation leads to the overproliferation or survival of several cancer cells, such as basal cell carcinoma or B-cell lymphomas.[13–15] There are some HH inhibitors under clinical trial as drug candidates against those cancers.[16]

In the present study, using ATL patient samples and some ATL models, we found two specific gene overproductions in ATL, *Ellis Van Creveld syndrome 1* (*EVC1*) and *EVC2*, which belong to the EVC family of genes that are implicated in HH regulation.[17–19] We demonstrated that epigenetically upregulated EVC was associated with cellular HH activity. *EVC* and other regulatory factors for HH signaling were responsible for the survival of ATL cell lines and also primary ATL samples. Direct evidence from the ATL samples revealed that universal epigenetic marks associated with actively transcribed genes were rearranged in the leukemic cells. These findings may shed light on the abnormal gene expression signature and leukemic cell traits observed in ATL.

Materials and Methods

Patient samples. The primary peripheral blood mononuclear cells (PBMC) from ATL patients and healthy volunteers were a part of those collected with informed consent as a collaborative project of the Joint Study on Prognostic Factors of ATL Development (JSPFAD). The project was approved by the University

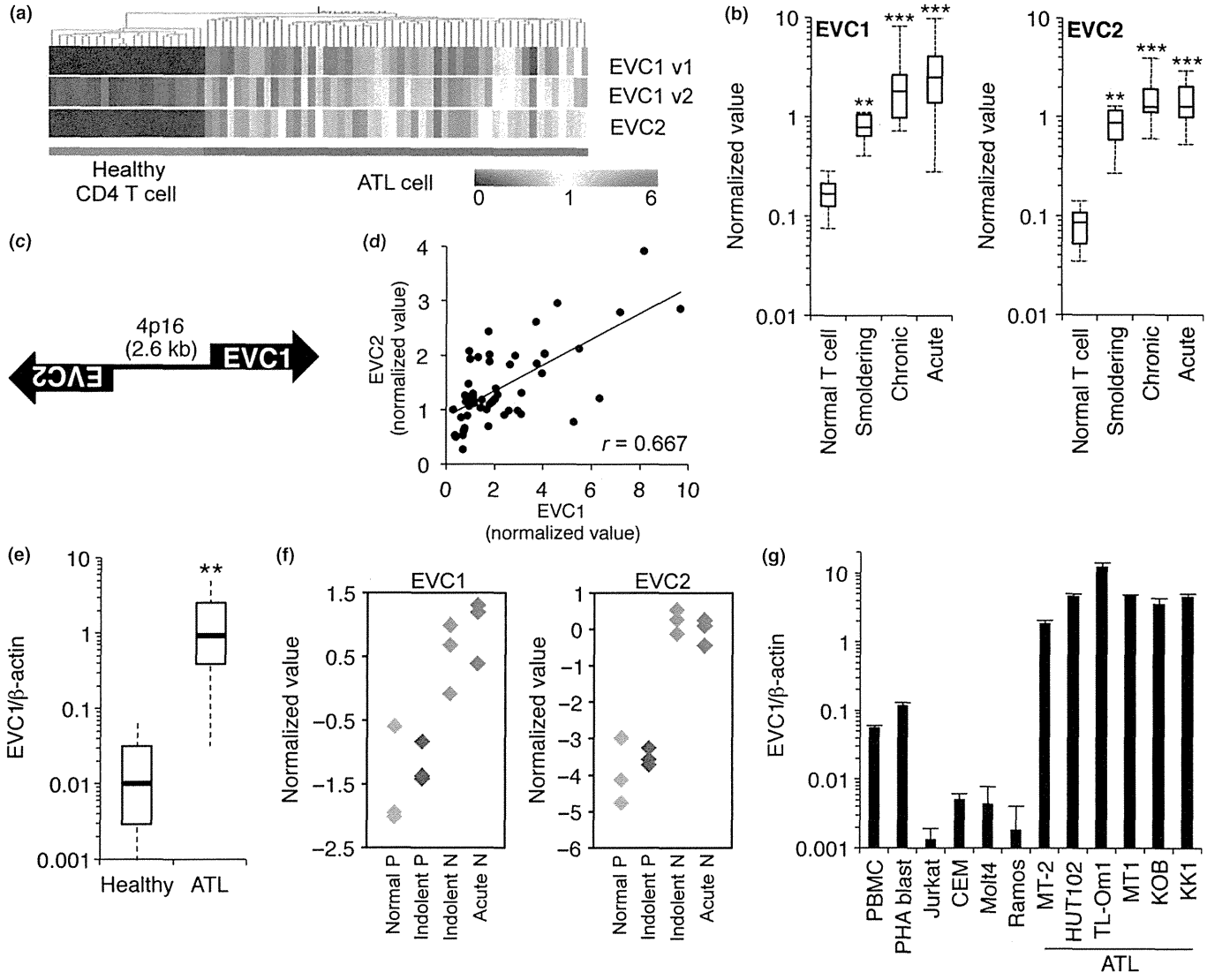

Fig. 1. *EVC* overexpression in ATL. (a, b) Microarray heatmap (a) and box plot (b) of *EVC*. $^{**}P < 0.01$. $^{***}P < 0.001$. (c) Schematic illustration of locus encoding *EVC1/2*. (d) Individual expression values ($n = 52$) between *EVC1* and *EVC2*. (e) *EVC1* mRNA level in ATL patient PBMC (total, $n = 11$; acute, $n = 7$; chronic, $n = 4$) and in CD4+ T cells from healthy donors ($n = 6$) evaluated using quantitative RT-PCR (qRT-PCR). $^{**}P < 0.01$. (f) *EVC1* and *EVC2* levels in CADM1 versus CD7 plot subpopulations. Normal P, CD4+/CADM1−/CD7+ T cells from healthy donors; Indolent P, CD4+/CADM1−/CD7+ from indolent ATL patients; Indolent N, CD4+/CADM1+/CD7− from indolent ATL patients; Acute N, CD4+/CADM1+/CD7− from acute ATL patients. The gene expression microarray dataset is available in Kobayashi *et al.*[25] (g) *EVC1* levels in various cell lines examined using qRT-PCR ($n = 3$, mean ± SD).

of Tokyo and Showa University research ethics committees. The PBMC were isolated using Ficoll separation and maintained in RPMI1640 (Invitrogen, Carlsbad, CA, USA) supplemented with 1% of self-serum and antibiotics (Invitrogen). Clinical information is shown in the Supporting Information Methods.

Microarray analysis. Gene expression profiling of ATL patient samples and normal CD4+ T cells has been performed previously.[5] The coordinate has been deposited in the Gene Expression Omnibus database (GSE33615).

Cell culture. The HTLV-1-infected cell lines MT-2 and HUT102, ATL-derived cells MT-1 and TL-Om1, and other leukemic cell lines were cultured in RPMI1640 with 10% FCS. ATL-derived KOB and KK1 were cultured in RPMI1640 with 10% FCS and 10 ng/mL recombinant human IL-2 (R&D Systems, Minneapolis, MN, USA). The 293T cell was cultured in DMEM with 10% FCS. All cell lines were cultured at 37°C, with 5% CO_2.

Plasmids and HH activity analysis. Tax-encoding plasmids have been described previously.[20] *EVC1* cDNA was amplified as two fragments from the human cDNA library. Cellular HH activity was evaluated using a dual-luciferase assay (Promega, Madison, WI, USA).[21] Briefly, 7 × GLI binding site (GACACCCA)-luciferase plasmid and control RSV-Renilla plasmid were co-transfected into target cells using Lipofectamine2000 (Invitrogen). At 24 h post-transfection, the cells were collected and analyzed using a dual-luciferase assay.

Quantitative RT-PCR. Procedures for RNA isolation and RT-PCR have been described previously.[5] Primer sets for quantitative RT-PCR (qRT-PCR) are provided in the Supporting Information Methods.

Epigenetic analyses. Bisulfite treatment was conducted using a MethylEasy Xceed Rapid DNA Bisulphite Modification kit (Human Genetic Signatures, NSW, Australia). For evaluating histone covalent modifications, a chromatin immunoprecipita-

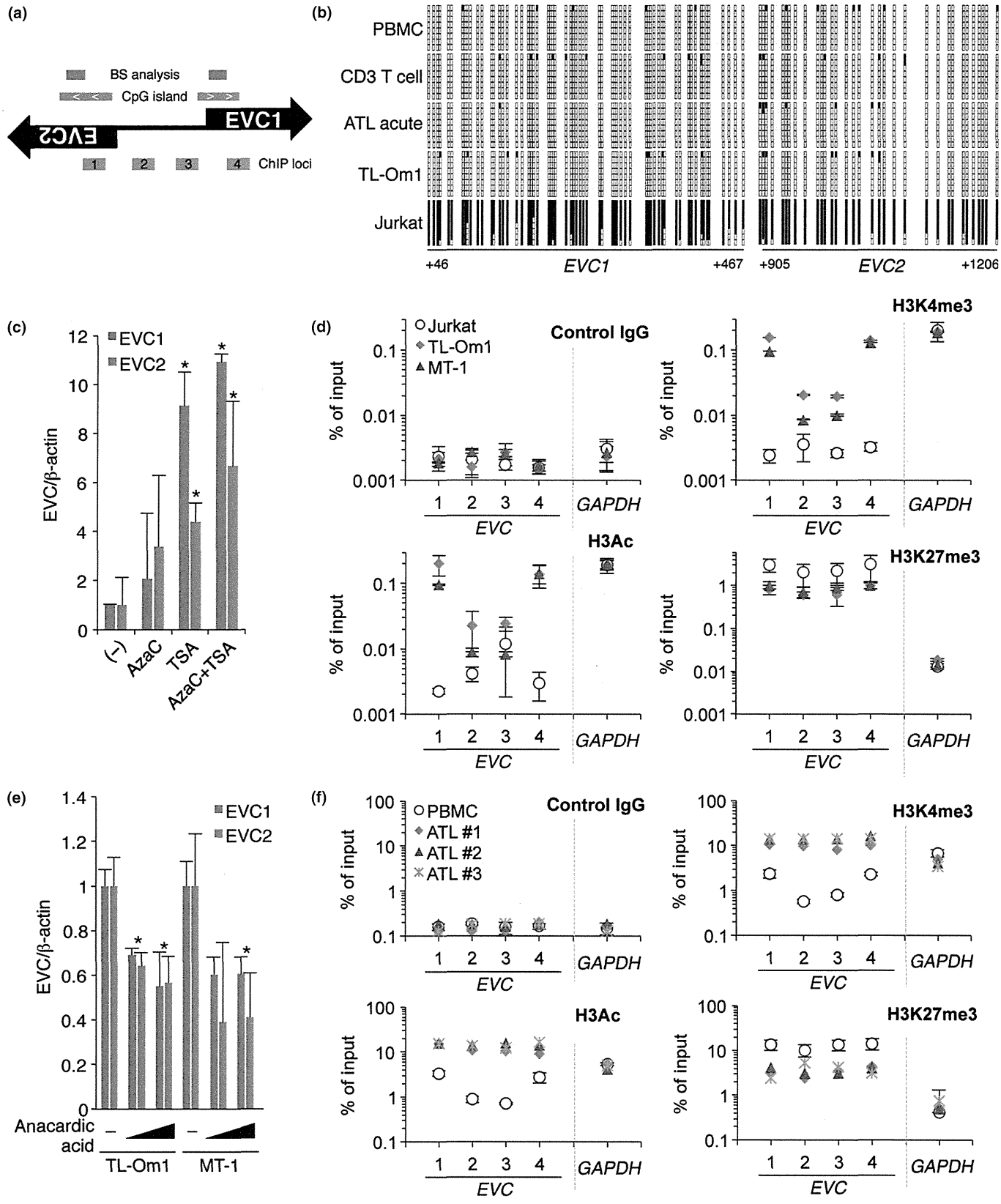

Fig. 2. Epigenetic reprogramming in the *EVC* locus. (a) Schematic of CpG islands and chromatin immunoprecipitation (ChIP) loci. (b) Results of bisulfite sequencing (+46 to +466 from *EVC1* transcription start site [TSS]; +905 to +1206 from *EVC2* TSS). The black and empty boxes represent methylated and unmethylated CpG, respectively. (c) *EVC* RNA levels in Jurkat cells in the presence or absence of epigenetic drugs ($n = 3$, mean ± SD). *$P < 0.05$. (d) Histone covalent modifications at *EVC* and *GAPDH* loci in three cell lines were analyzed using PCR-based ChIP assay with specific antibodies. Positions of primer sets for the real-time PCR are indicated in (a). Enrichment values relative to input samples are plotted. (e) TL-Om1 and MT-1 cells were treated with 1 or 5 μM of anacardic acid for 48 h and the *EVC* mRNA level was then analyzed ($n = 3$, mean ± SD). *$P < 0.05$. (f) Epigenetic changes in primary ATL samples. Three independent clinical samples were compared with normal PBMC ($n = 3$, mean ± SD).

tion (ChIP) assay was conducted as described previously.[5,22] Anti-H3K4me3 (#9751S; Cell Signaling, Danvers, MA, USA), anti-AcH3 (#06-599; Millipore, Billerica, MA, USA), anti-H3K27me3 (#39155; Active Motif, Carlsbad, CA, USA) and control IgG (I5381; SIGMA, St. Louis, MO, USA) were used for ChIP. Primers for the qPCR are provided in the Supporting Information Methods.

Immunohistochemistry. For preparation of the paraffin block of 293T cells, the cells were fixed in 20% of formalin/PBS for 24 h. After removing the formalin, alcohol dehydration and paraffin permeation were done using Tissue-Tek VIP5Jr (Sakura, Alphen aan den Rijn, The Netherlands). Paraffin blocks were sectioned at 3-μm thickness. The sections were then transferred to coating slide glasses (Muto pure chemicals, Bunkyo-ku, Tokyo, Japan). After paraffin removal, the paraffin sections of the 293T and ATL cells were treated with 3% H_2O_2. Antigen-retrieval treatment was done using Histofine antigen retrieval solution pH9 (Nichirei, Chuo-Ku, Tokyo, Japan) for 20 min under microwave radiation. After reaction with the first antibody, anti-EVC antibody (HPA008703, 1:400; SIGMA), and the second antibody (K5027, ENVISION Kit/HRP [DAB]; Dako, Bunkyo-ku, Tokyo, Japan), the sections were colored using ENVISION Kit/HRP [DAB] DAB+ (K3468; DAKO). Finally, the sections were stained with hematoxylin.

Lentivirus construction and production. Detailed procedures for lentivirus production have been described previously.[5] Briefly, replication-defective, self-inactivating lentivirus vectors were used.[23,24] shRNA were cloned into a CS-H1-EVBsd. High-titer viral solutions prepared using a centrifugation-based concentration were transduced into ATL cell lines using the spinoculation method. The transduced cells were

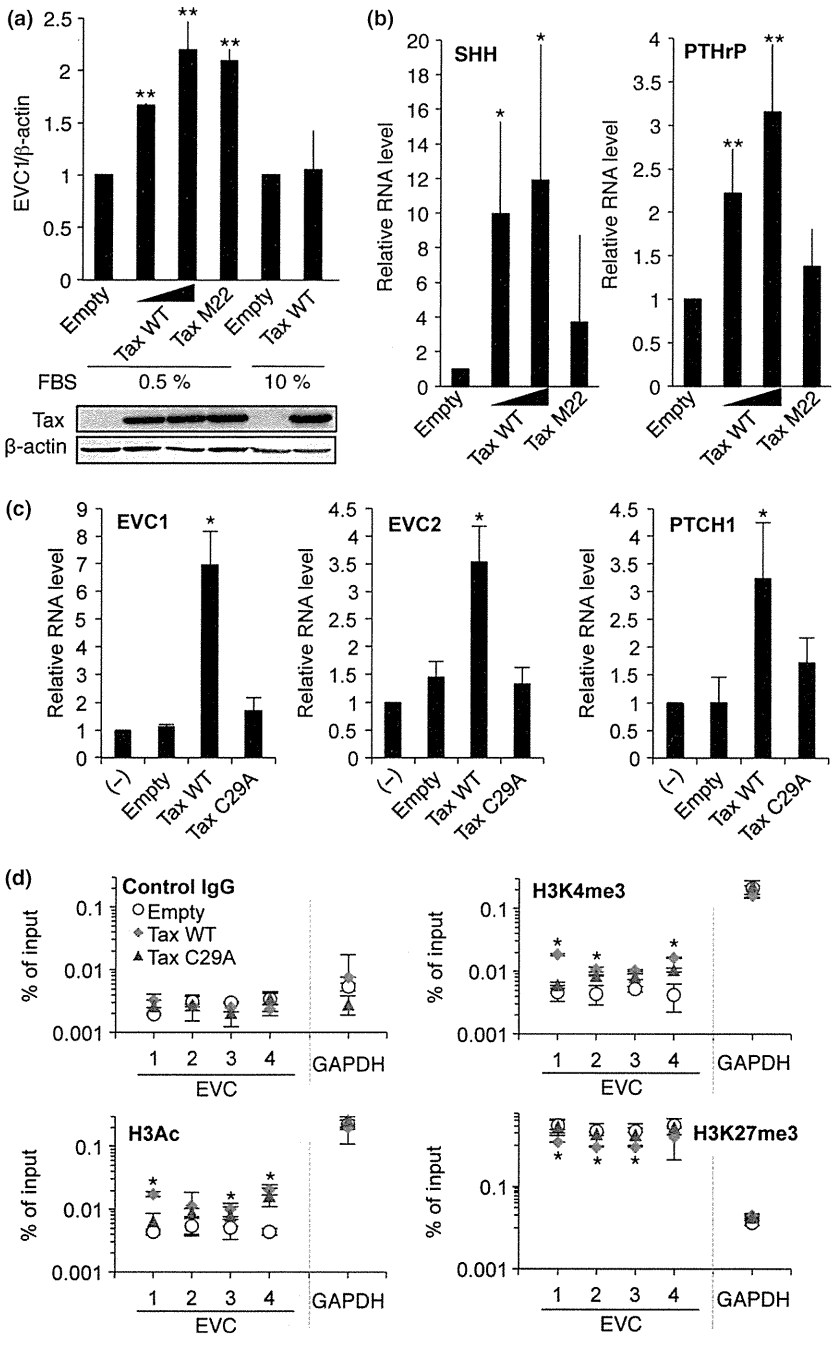

Fig. 3. Role of Tax in *EVC* regulation. (a) *EVC1* RNA levels are affected by Tax. The 293T cells in different FBS condition were transfected with the indicated plasmids. Relative *EVC1* levels were evaluated using quantitative RT-PCR (qRT-PCR) (top panel, $n = 3$, mean ± SD). $^{**}P < 0.01$. Tax expression was confir-med using western blotting with an anti-Tax antibody (Lt-4) (bottom panel). (b) Levels of *SHH* and *PTHrP* in the presence or absence of Tax ($n = 3$, mean ± SD). $^{*}P < 0.05$. $^{**}P < 0.01$. (c) *EVC* and *PTCH1* levels in Jurkat cells expressing Tax ($n = 3$, mean ± SD). $^{*}P < 0.05$. (d) Tax-mediated epigenetic changes. Histone modifications at *EVC* and *GAPDH* loci in Tax-expressing Jurkat cells were analyzed using a ChIP assay. $^{*}P < 0.05$ (Tax WT *vs* Empty). Primer positions are shown in Figure 2(a).